Displacement-Based Design of Geosynthetic-Reinforced Pile-Supported Embankments to Increase Sustainability

(article starts on next page)

Displacement-Based Design of Geosynthetic-Reinforced Pile-Supported Embankments to Increase Sustainability

Viviana Mangraviti

Abstract Although the construction of concrete piles has a relevant environmental footprint, they are commonly used to reduce settlements of embankments on soft soil strata. A more sustainable choice to further reduce settlements (and, consequently, the number of piles) is to place geosynthetics below the embankment. However, existing design methods cannot calculate settlements at the embankment top and cannot be used to optimise the number of piles in a displacement-based design. In this note, an innovative model for assessing settlements at the top of Geosynthetic-Reinforced and Pile-Supported embankments induced by the embankment construction process is presented and validated against finite difference numerical analyses. The model is used to optimise the design of both piles and geosynthetic, and applied to a practical example, where the mass of CO_2 saved by designing geosynthetics to reduce the pile number.

Graphical Abstract
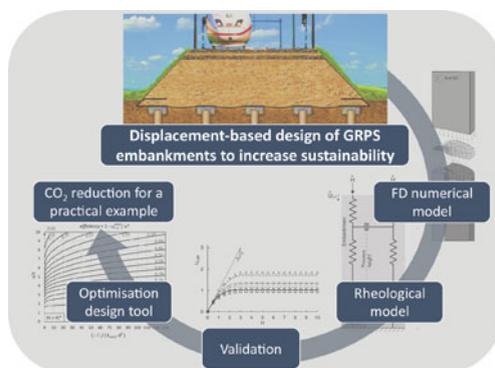
Keywords Geosynthetic-reinforced and Pile-Supported embankments · Displacement-based · SDG 9 · Sustainability · CO_2

V. Mangraviti (✉)
Chalmers University of Technology, 412 96 Gothenburg, Sweden
e-mail: viviana.mangraviti@chalmers.se

1 Introduction

The expansion of urban areas featuring the last century resulted in the exploitation of increasingly large areas of territory, leading to deleterious impacts on the environment. Civil engineering is immensely contributing to the consumption of global energy reserves along with the severe exploitation of raw materials such as gravel, sand, and water [1]. Furthermore, the greenhouse gas emissions due to the production of concrete structures compared to both steel and wood structures is the highest [2]. For this reason, at least 2 of the 17 Sustainable Development Goals (SDGs) defined by United Nations (UN) in 2015 (i.e. both SDGs 9, "industry, innovation and infrastructures", and 11, "sustainable cities and communities", in Johnston [3]) can be linked to civil engineering.

In a context where all engineers can have a major influence towards a more sustainable development, geotechnical engineering has a crucial role in influencing the sustainability of a project. In fact, according to Abreu et al. [4], geotechnical engineering is one of the key contributing fields to sustainable development, since it faces a challenging dichotomy between delivering project goals (environmental, economic, and social) and maintaining sustainability. In fact, from a practical point of view, the exploitation of increasingly large areas of territory has led also to the construction of infrastructures under difficult geological and geotechnical conditions, requiring geotechnical engineers to find new and not always "environmentally friendly" solutions. As an example, embankments for major infrastructures are more often realised in areas where soils are deformable, and to avoid unacceptable settlements, concrete piles are commonly employed as settlement reducers. Such "geo-structures", composed by embankment, foundation soil and concrete piles, are named Conventional Pile-Supported (CPS) embankments. The rigid inclusion induces the development of the "arching effect" within the embankment soil, reducing the portion of embankment load transferred to the soft soil, while stresses flow towards the piles, and consequently alleviating differential settlements. Depending on both the overall length of the infrastructure to be realised and the mechanical properties of the ground to improve, CPS embankments may require the installation of a huge number of concrete piles along different kilometres of infrastructure, leading to a huge outflow of both economic and environmental resources.

To further reduce settlements at the top (where infrastructures are placed) of CPS embankments, geosynthetic layers can be placed below the embankment. In the literature, Geosynthetic-Reinforced and Pile-Supported (GRPS) embankments were studied by several authors [5–11], and geosynthetics were found to effectively increase the transfer loads towards the piles, leading to several advantages: (i) a decreased number of inclusions (piles) needed; (ii) faster construction, and (iii) better control of differential settlements associated with soft soils. As a consequence, for equal admissible settlements at the embankment top, GRPS embankments need a fewer number of piles than CPS embankment, reducing the Embodied Carbon (EC, referring to carbon dioxide emitted during the manufacturing, transport, construction and the "end of life" of a material) due to the use of concrete.

Unfortunately, due to the lack of simplified methods, nowadays the design of GRPS embankments under a displacement-based perspective can only be done by using advanced numerical methods. In fact, the current design guidelines for GRPS embankments issued by several countries [12–15], adopt approaches based on the limit-equilibrium method that are not suitable neither to estimate settlements at the top of the embankment nor to ensure the serviceability of the geo-structure over its all lifetime [16]. In fact, these equilibrium arching models could possibly lead to an overestimation of the number of piles needed representing, from a sustainability perspective, a waste of both energy and resources. Nevertheless, to reach SDG 9, a more sustainable design perspective needs to be developed and spread in the next years.

With the aim of providing a more effective displacement-based design tool for GRPS embankments, Mangraviti et al. [11, 17] proposed an upscaled constitutive relationship to evaluate both differential and average settlements at the top of the central part of the embankment. The model was conceived as an extension of the one proposed by di Prisco et al. [18] for CPS embankments and derives from the interpretation of the results of a series of Finite Difference (FD) numerical analyses focusing on the construction process under drained conditions of the embankment.

In this chapter, the GRPS embankments capability to deform less than CPS embankments is firstly discussed by means of FD numerical results, expressed in terms of evolution of both average and differential settlements at the top of the embankment during construction. The upscaled constitutive relationship from Mangraviti et al. [17] is then shortly described and used as a tool to optimise the design of both piles and geosynthetic layer in a direct displacement-based perspective. Optimise the design means to employ the number of piles strictly necessary to undergo an admissible settlement at the top and, therefore, to achieve a more sustainable design, reducing EC.

The text is structured as it follows: in Sect. 1 the FD numerical model is presented and the results for both CPS and GPRS embankments are discussed. In Sect. 2 the constitutive relationship is briefly introduced and compared against numerical results. In Sect. 3 a non-dimensional chart to optimise the design of both piles and geosynthetics is provided and used to solve a practical example, where the EC for both CPS and GRPS embankments are calculated and compared.

2   Numerical Model

In the most general case, the design of both CPS and GRPS embankments is a three-dimensional problem. Nevertheless, when the embankment transversal width is significantly larger than its height, side effects may be disregarded and only one central axisymmetric cell can be considered as representative of the mechanical behaviour of the central part of system (Fig. 1a). The cell, whose diameter is equal to the spacing (s) between piles, includes: (*i*) the pile of length *l* and diameter *d*, (*ii*) the soft foundation soil, (*iii*) the embankment, whose height, *h*, evolves during
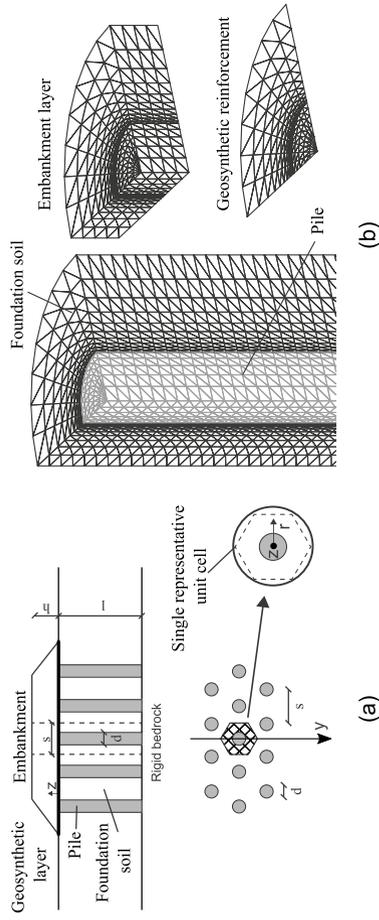
Fig. 1 **a** Problem geometry and representative axisymmetric cell; **b** numerical model

construction and (*iv*) the geosynthetic layer. The origin of both radial and vertical coordinates (*r* and *z* respectively) is in the centre of the pile top (Fig. 1a).

The problem has been numerically modelled by means of the finite difference numerical code FLAC3D [19]. Due to axisymmetry, only one quarter of the representative cell has been considered (Fig. 1b). The concrete end-bearing has been modelled as an elastic element. The mechanical behaviour of both the embankment and the foundation soil was modelled by means of an elastic-perfectly plastic constitutive relationship with a Mohr-Coulomb failure criterion and a non-associated flow rule. An elastic membrane element, characterised by axial stiffness *J*, has been used to model the reinforcement. When $J = 0$, the case of CPS embankment is obtained. Smooth interface elements were introduced between the pile and the foundation soil, whereas frictional interface elements were used between the geosynthetic and the soil. Normal displacements are not allowed on the lateral boundary and at the base of the domain.

To reproduce the construction process of the embankment, the numerical analysis has been subdivided in several stages. Each stage corresponds to the construction of 25 cm thick layer of the embankment under drained conditions. Therefore, the geometry of the spatial domain progressively evolves, adding at each stage a new layer of elements at the top of the model.

Even though a parametric study was conducted [11], for the sake of brevity, the results concerning only one reference geometry ($s = 1.5$ m, $d = 0.5$ m and $l = 5$ m) for different values of geosynthetic axial stiffness are hereafter illustrated in order to highlight the effectiveness of the geosynthetic layer in reducing settlements at the top of the embankment. The mechanical parameters used for the reference case are reported in Table 1. The dilatancy angle was found not to affect the mechanical processes of the system, although a slightly decrease in both average and differential settlements is observed within the embankment (the results are here omitted for the sake of brevity).

During the first step of construction, plastic strains develop in a narrow zone close to the top corner of the pile (defined as "process zone" in [18, 20], see Fig. 2). The evolution of this yielded zone is described by the process height h_p and when $h_p = h^*$ the plastic zone stops evolving.

According to di Prisco et al. [18], the mechanical response of the geo-structure can be described by using the following non-dimensional variables:

Table 1 Mechanical properties for the reference case

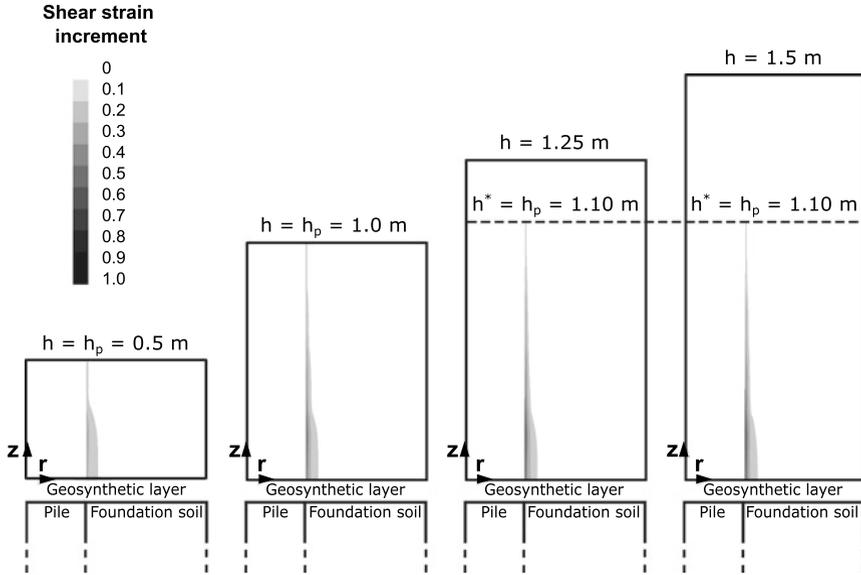|	Unit weight (kN/m^3)	Young's modulus (MPa)	Poisson's ratio (–)	Friction angle (°)	Dilatancy angle (°)
Foundation soil	18	1	0.3	30	0
Embankment	18	10	0.3	40	0
Pile	25	30000	0.3	–	–

Fig. 2 Evolution of shear plastic strain during the construction process

$$H = h/d \tag{1}$$

$$U_{t,p} = \frac{u_{t,p}}{d} \frac{E_{\mathrm{oed},f}/l}{\gamma} \quad \text{and} \quad U_{t,f} = \frac{u_{t,f}}{d} \frac{E_{\mathrm{oed},f}/l}{\gamma} \tag{2}$$

$$U_{t,\mathrm{diff}} = U_{t,f} - U_{t,p} \quad \text{and} \quad U_{t,\mathrm{av}} = \frac{U_{t,f}(S^2 - 1) + U_{t,c}}{S^2} \tag{3}$$

where $u_{t,\blacksquare}$ are the average displacement at the top of the embankment, being the subscripts $\blacksquare = p$ and f when referring to pile (i.e. settlements and stresses for $0 < r < d/2$) and foundation soil ($d/2 < r < s/2$) respectively. $U_{t,\mathrm{diff}}$ and $U_{t,\mathrm{av}}$ are the non-dimensional differential and average settlements at the top; $S = s/d$ is the non-dimensional spacing; $E_{\mathrm{oed},f}$ is the foundation soil oedometric modulus and the embankment unit weight.

The numerical results in Fig. 3 are plotted in non-dimensional planes where the system response was found to be uniquely defined if the non-dimensional geometrical ratios ($S = s/d$, $L = l/d$), the non-dimensional stiffness ratio ($E_{\mathrm{oed},e}/E_{\mathrm{oed},f}$, being $E_{oed,e}$ the embankment soil oedometric modulus) and the embankment soil failure parameters (friction, ϕ'_e, and dilatancy angle, ψ_e, values) are kept constant. Due to the high difference in stiffness between piles and surrounding soil, differential settlements developing at the embankment base propagate to the top ($U_{t,\mathrm{diff}} > 0$ in Fig. 3a). When H is sufficiently large ($H = H^* = h^*/d$, i.e. values highlighted with filled black rectangles in Fig. 3), differential settlements at the top of the embankment

stop increasing, whereas average settlements continuously increase (Fig. 3b). As a consequence, any increase in load (e.g. the construction of the infrastructure above the embankment) for $H > H^*$ will not induce any increment of differential settlement in the transversal direction (r in Fig. 1), meaning that H^* in $r - z$ plane coincides with the height of the "plane of equal settlements", defined as the locus where the increment of differential displacements is negligible. On the contrary, $U_{t,\mathrm{av}}$ continues to increase even for $H > H^*$, meaning that differential settlements in the longitudinal (y in Fig. 1a) direction increase. Therefore, H^* is a fundamental value to define the mechanical behaviour of the system when further loaded.

Due to the definition of non-dimensional variables (Eq. 3), the dashed lines inclined 1:1 in Fig. 3a,b represent the case of pile stiffness coincident with the foundation soil one and of $J = 0$ (i.e. nor piles neither geosynthetic are placed). The distance between $U_{t,\mathrm{av}}$ and the 1:1 line is a measure of the effectiveness of both piles and geosynthetics as settlements reducers. The presence of the geosynthetic further reduce settlements with respect to the $J = 0$ case (Fig. 3a, b) meaning that, given a fixed value of settlement, less piles are needed when a geosynthetic layer with larger J is used. A direct connection between pile spacing (strictly related to the number of piles) and geosynthetic stiffness will be discussed in Sect. 3.

3 Mathematical Model

In di Prisco et al. and Mangraviti et al. [10, 11, 21] the critical interpretation of numerical results for GRPS embankments lead to the identification of 6 subdomains (Fig. 4a). All the subdomains are considered as elastic and behave in pseudo-
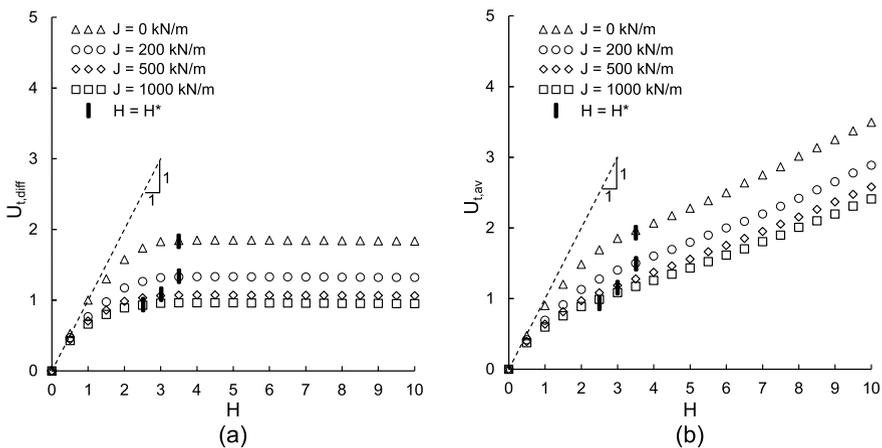
Fig. 3 Numerical results during embankment construction in terms of non-dimensional, **a** differential and **b** average settlements at the top of the embankment for different values of the geosynthetic axial stiffness
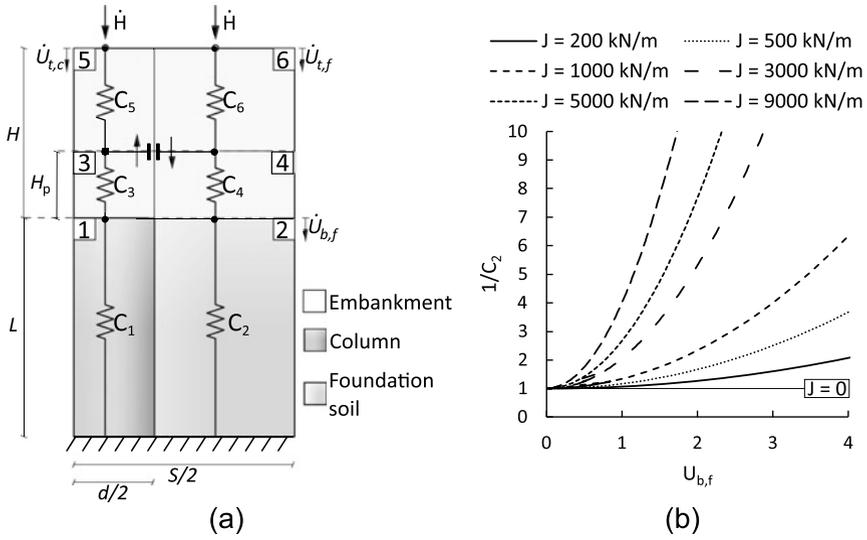
Fig. 4 **a** Rheological model for CPS embankments; **b** stiffness of reinforced foundation soil versus embankment base displacement for different J

oedometric conditions, whereas the arching effect [11, 17] is modelled as localised at the interface between subdomains 3 and 4. The mechanical behaviour of each subdomain can be reproduced by means of elastic springs and the arching effect is considered as localised and represented by a frictional slider placed in $z = H_p$ and $r = d/2$. In Fig. 4a, the non-dimensional compliances C_1 and C_2 represent the pile and the reinforced foundation soil respectively, whereas C_3 and C_4 are the compliances related to the portion of embankment H_p thick. Due to the evolution of H_p (Fig. 2) with the loading function $\dot{H}$, subdomains 3 and 4 evolves during construction. $C_5 = C_6$ is the compliance of the soil stratum $(H-H_p)$ thick. Due to the definition of non-dimensional quantities, $C_2 = 1$ when $J = 0$, whereas, when $J \neq 0$, C_2 is a function of non-dimensional settlement at the embankment bottom, $U_{b,f}$ (i.e. geosynthetic deformation). As a consequence, when $J = 0$, the model for GRPS embankments [11, 17] reduces to the one for CPS ones [18]. The equation describing the evolution of the non-dimensional stiffness $1/C_2$ with $U_{b,f}$ was numerically calibrated and the curves for different values of J are reported in Fig. 4b.

To evaluate settlements at the top of both CPS and GRPS embankments, an incremental relationship between the generalised loading variable $\dot{H}$ and the displacements at the top of the embankment $U_{t,\text{diff}}$ and $U_{t,\text{av}}$ was conceived:

$$\begin{bmatrix} \dot{U}_{t,\text{diff}} \\ \dot{U}_{t,\text{av}} \end{bmatrix} = \begin{bmatrix} C_{\text{diff}} \\ C_{\text{av}} \end{bmatrix} \dot{H} \tag{4}$$

C_{diff} and C_{av} represent the non-dimensional compliances of the overall system, analytically evaluated by (i) employing the rheological scheme illustrated in Fig. 4a; (ii) imposing the balance of momentum and compatibility conditions along the vertical direction; (iii) imposing the definition of plane of equal settlements ($\dot{U}_{t,\text{diff}} = 0$).

The obtained constitutive model in Eq. (4), describing the response of GRPS embankments depends on: (i) the mechanical parameters of piles, soil (Table 1) and geosynthetic (J); (ii) the geometrical variables (s, d, l) and (iii) the average ratio between horizontal and vertical stresses (k) in the portion of embankment in which irreversible strains accumulated. According to di Prisco et al. [18], k is the only parameter of the model which is not directly related on the system geometry/mechanical properties. k is not significantly affected by J [11] but only depends on the dilatancy angle.

A conservative value of the final height of the plane of equal settlements can be estimated as (di Prisco et al. [18]):

$$H^* = \frac{1}{2}\sqrt{\left[\frac{E_{\text{oed},e}}{E_{\text{oed},f}}\frac{L}{S^2}C_2\right]^2 + \frac{(S^2-1)}{\bar{k}\tan\phi'_{ss}}\left(\frac{E_{\text{oed},e}}{E_{\text{oed},f}}\frac{L}{S^2}\right)C_2} - \frac{1}{2}\left(\frac{E_{\text{oed},e}}{E_{\text{oed},f}}\frac{L}{S^2}\right)C_2 \quad (5)$$

As previously mentioned, for GRPS embankments C_2 in Eq. (5) is a function of $U_{b,f}$ and, according to the trend reported in Fig. 4b, the critical height H^* decreases for larger values of the geosynthetic axial stiffness J (i.e. H^* is maximum when $J = 0$). Eq. (5) will be used in the following section as a key ingredient to optimise the design of GRPS embankments.

The results obtained by integrating the mathematical model in Eq. (4) are compared with the numerical ones (see Fig. 3) in Fig. 5, where a good agree-
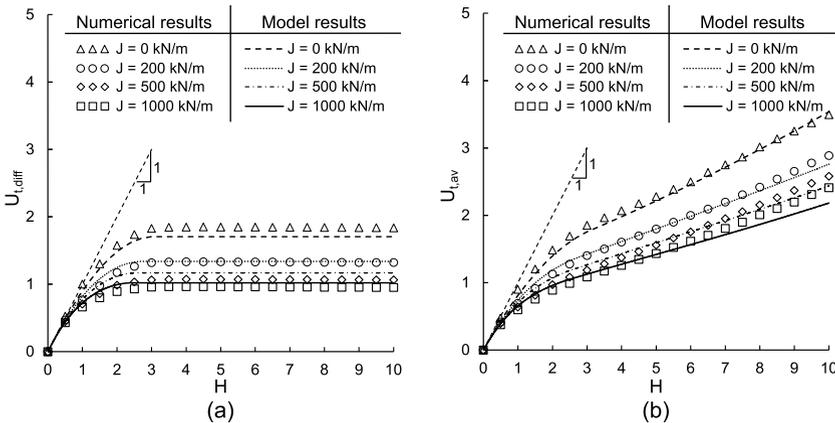
Fig. 5 Comparison between non-dimensional numerical results and the mathematical model in Eq. (4) in terms of **a** differential and **b** average settlements at the top of the embankment

ment is obtained for each value of J in terms of both differential (Fig. 5a) and average (Fig. 5b) settlement. The comparison between the mathematical model and the numerical results from a parametric study showed a satisfactory agreement [11], but the results are here omitted for brevity.

4   Optimisation of GRPS Embankments Design to Increase Sustainability and Practical Example

From a practical point of view, geotechnical engineers should design both piles (i.e. l, s and d) and geosynthetic layer (i.e. J) in order to have an average settlement at the top of GRPS embankments lower than an admissible settlement ($u_{t,\mathrm{av}}^{\mathrm{amm}}$). If end-bearing piles are considered, l is known, as well as the mechanical properties of the soft soil ($E_{\mathrm{oed},f}$).

Settlements accumulated during embankment construction are generally levelled thanks to the rollers compacting the soil. However, it is important that, after the construction of the infrastructure (i.e. either road superstructure or ballast plus rail track, where the rollers cannot be used anymore), the embankment does not settle more than expected. In fact, that would lead to possibly dangerous consequences to people and expensive damages to the infrastructure. As previously shown in Sects. 1 and 2, when $H > H^*$, differential settlements in r-direction stop increase (Fig. 5a), whereas average settlements (i.e. differential settlements in y-direction) continuously increase (Fig. 5b). As a consequence, to design GPRS embankments with a displacement-based approach, it is important: (i) that the final height of the embankment is larger than H^*, in order to avoid an increase in $U_{t,\mathrm{diff}}$ and (ii) that the value of $U_{t,\mathrm{av}}$ is equal or lower than the admissible one.

In this perspective, the rheological model in Eq. (4) was integrated and used to solve an optimisation problem: the maximum value of $S = s/d$ was evaluated, for several values of non-dimensional $J^* = (Jl)/(E_{\mathrm{oed},f}\, d^2)$ and for fixed values of the following non-dimensional efficiency: $1 - u_{t,\mathrm{av}}^{\mathrm{amm}}/u^*$, where:

$$u^* = \Delta q \left(l/E_{\mathrm{oed,f}} + 0.5\Delta h/E_{\mathrm{oed,e}} \right) \tag{6}$$

is the settlement at the embankment top induced by the load $\Delta q = \gamma \Delta h$ when nor piles neither geosynthetic are installed. Δq is the distributed load representative for the infrastructure weight, being Δh the thickness of embankment equivalent to the construction of the infrastructure layer ($\Delta h = \gamma_i \Delta h_i/\gamma$ being γ_i and Δh_i the unit weight and the thickness of the infrastructure respectively). Several curves were obtained (Fig. 6) for fixed ϕ'_e and ψ_e, and for $H > H^*$, where a safe side estimation of H^* can be determined by substituting $C_2^r = 1$ in Eq. (5). For the sake of safety, the curves were obtained by considering $u_{\mathrm{t,av}}^{\mathrm{amm}}$ equal to the maximum increment of average settlements at the top of the embankment (Eqs. 4, 3, 2) for $H > H^*$.

Fig. 6 Non-dimensional efficiency isolines for optimisation of GRPS embankments preliminary design (for $H > H^*$, $\phi'_e = 40°$ and $\psi_e = 0$)
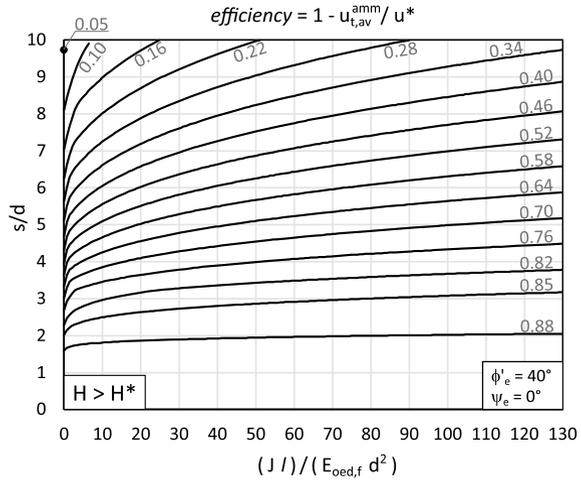
$1 - u_{t,\mathrm{av}}^{\mathrm{amm}}/u^*$ is a measure of the efficiency of the installation of both piles and geosynthetic: it will be equal to 0 when $u_{t,\mathrm{av}}^{\mathrm{amm}} = u^*$, whereas it is 1 for $u_{t,\mathrm{av}}^{\mathrm{amm}}/u^* \to 0$. As expected, by increasing the axial stiffness of the geosynthetic layer, a larger pile spacing can be chosen, possibly leading to a reduction of the concrete piles number and to a more sustainable design. However, it is worth noticing that, since the geosynthetic is more effective in transferring stresses to the piles when it deforms more (i.e. larger settlements), for large $u_{t,\mathrm{av}}^{\mathrm{amm}}/u^*$ values (i.e. low values of the efficiency in Fig. 6) the curves are more inclined and a small increase in J^* lead to choose piles with larger spacing (or smaller diameter). On the contrary, when very small settlements are admitted (i.e. larger efficiency is required), the increase in J^* induces small increase in s/d.

As an example, a GRPS embankment, with 25 m central part in r-direction, can be considered to be realised over a 5 m thick soft soil stratum (i.e. $l = 5$ m). The mechanical properties of the foundation soil, the concrete pile and the embankment soil are those reported in Table 1. A differential settlement of 6 mm at the top of the embankment is considered as admissible after a $\Delta h_i = 50$ cm thick superstructure is constructed. For the sake of simplicity, in this case, the unit weight of the infrastructure is (conservatively) assumed to be equal to the one of the embankment soil ($\gamma_i = \gamma \rightarrow \Delta q = \gamma_i \, \Delta h_i = 18 \cdot 0.5 = 9$ kPa).

As a first step, the isoline with *efficiency* $= 1 - (0.006)/[(9) \cdot (5/1346 + + 0.5 \cdot 0.5/13462)] = 0.82$ is individuated in Fig. 6. All the $s/d - Jl/(E_{\mathrm{oed},f} \, d^2)$ couples on the 0.82 isoline can be chosen to have a settlement at the top of the embankment equal to the admissible settlement (6 mm). In order to optimise both environmental and economic resources, the designer should look for the maximum values of both s and J that better suits the project needs.

To estimate the increment in sustainability (i.e. the reduction in CO_2 emissions) induced by considering a GRPS embankment instead of a CPS one, both $J = 0$ and J

Table 2 Example of design optimization: piles number and tCO_2 for CPS and GRPS embankment

Embankment	J (kN/m)	s (m)	Piles number	Piles (tCO_2)	Geogrid (tCO_2)	Total (tCO_2)
CPS	0	1.1	23	60.55	0	60.55
GRPS	1000	1.5	17	45.74	0.05	45.79

$= 1000$ kN/m were considered. By assuming a first tentative value of pile diameter equal to 0.5 m, s is estimated from Fig. 6 and the corresponding number of piles to be placed in the central part (25 m in r-direction) of the embankment are evaluated and reported in Table 2. To evaluate the tons of CO_2 saved by realizing 17 piles and the geosynthetic layer (instead of 23 piles), the EC for both concrete and geosynthetics is considered. EC is generally measured in mass of CO_2 emitted per mass of material. In particular, an average value of EC = $1.08tCO_2/t$ was chosen for the concrete (whose mass is 2500 kg/m^3) [22] and EC = $2.36tCO_2/t$ was considered for a woven geogrid (whose mass is 0.53 kg/m^2) [23]. The reduced number of piles employed for the GRPS embankment led to a 24% reduction of CO_2 emissions if compared to the CPS embankment. The same calculation may be repeated for a different value of d, in other to further optimise the sustainability of the project.

The charts in Fig. 6 represent a very effective and quick tool to design GRPS embankments in a displacement-based perspective and to optimise the number of piles for a more sustainable design. Several design charts were obtained for different ϕ'_e and ψ_e and are here omitted for the sake of brevity.

5 Conclusion

In this chapter a mathematical model capable of reproducing the mechanical response of GRPS embankments is presented. The model considers the embankment height as a generalised loading variable and allows to evaluate settlements at the top of the embankment during construction under drained conditions. The model is highly innovative since it represents an effective tool during the preliminary design of GRPS embankments, including a displacement-based approach. In order to move a step forward towards a more sustainable construction of infrastructures (SDG 9) and reduce as much as possible the CO_2 emissions due to the construction of unnecessary concrete piles, one chart was provided to optimise the design of both piles and geosynthetic in a displacement-based perspective. The calculation of CO_2 saved for the practical example considered confirmed that GRPS embankments are a more sustainable choice if compared to CPS embankments.

References

1. Dixit, M.K., Fernández-Solís, J.L., Lavy, S., Culp, C.H.: Identification of parameters for embodied energy measurement: a literature review. Energy Build. **42**(8), 1238–1247 (2010). https://doi.org/10.1016/j.enbuild.2010.02.016
2. Latawiec, R., Woyciechowski, P., Kowalski, K.J.: Sustainable concrete performance—CO_2-emission. Environ. MDPI **5**(2), 1–14 (2018). https://doi.org/10.3390/environments5020027
3. Johnston, R.B.: Arsenic and the 2030 Agenda for sustainable development. In: Arsenic Research and Global Sustainability—Proceedings of the 6th International Congress on Arsenic in the Environment, AS 2016, pp. 12–14 (2016). https://doi.org/10.1201/b20466-7
4. Abreu, D.G., Jefferson, I., Braithwaite, P.A., Chapman, D.N.: Why is sustainability important in geotechnical engineering?, pp. 821–828 (2008). https://doi.org/10.1061/40971(310)102
5. Han, J., Gabr, M.A.: Numerical analysis of geosynthetic-reinforced and pile-supported earth platforms over soft soil. J. Geotech. Geoenviron. Eng. **128**(1), 44–53 (2002). https://doi.org/10.1061/(asce)1090-0241(2002)128:1(44)
6. Stewart, M.E., Filz, G.M.: Influence of clay compressibility on geosynthetic loads in bridging layers for column-supported embankments, pp. 1–14 (2005). https://doi.org/10.1061/40777(156)8
7. Yan, L., Yang, J.S., Han, J.: Parametric study on geosynthetic-reinforced pile-supported embankments. Adv. Earth Struct. 255–261 (2006). https://doi.org/10.1061/40863(195)28
8. Liu, H.L., Ng, C.W.W., Fei, K.: Performance of a geogrid-reinforced and pile-supported highway embankment over soft clay: case study. J. Geotech. Geoenviron. Eng. **133**(12), 1483–1493 (2007). https://doi.org/10.1061/(asce)1090-0241(2007)133:12(1483)
9. Wijerathna, M., Liyanapathirana, D.S.: Load transfer mechanism in geosynthetic reinforced column-supported embankments. Geosynth. Int. **27**(3), 236–248 (2020). https://doi.org/10.1680/jgein.19.00022
10. di Prisco, C., Flessati, L., Galli, A., Mangraviti, V.: A Simplified approach for the estimation of settlements of earth embankments on piled foundations. Lect. Notes Civil Eng. **40**, 640–648 (2020). https://doi.org/10.1007/978-3-030-21359-6_68
11. Mangraviti, V.: Theoretical modelling of embankments based on piled foundations. Ph.D. thesis, Politecnico di Milano (2021)
12. BSi.: BS 8006:1995—Code of practice for strengthened/reinforced soils and other fills Amd 1. British Standards Institution. ISBN 978-0-580-53842-1 (1995)
13. EBGEO.: Empfehlungen für den Entwurf und die Berechnung von Erdkörpern mit Bewehrungen aus Geokunststoffen—EBGEO (2010)
14. ASIRI.: Recommandations pour le dimensionnement, l'execution et le controle de l'amelioration des sols de fondation par inclusions rigides. ISBN 978-2-85978-462-1 (2012)
15. CUR226.: Design Guideline Basal Reinforced Piled Embankments. CRC Press (2016)
16. King, D.J., Bouazza, A., Gniel, J.R., Rowe, R.K., Bui, H.H.: Serviceability design for geosynthetic reinforced column supported embankments. Geotext. Geomembr. **45**(4), 261–279 (2017). https://doi.org/10.1016/j.geotexmem.2017.02.006
17. Mangraviti, V., Flessati, L., di Prisco, C.: Mathematical modelling of the mechanical response of Geosynthetic-Reinforced and Pile-Supported embankments. Under Rev. (2022)
18. di Prisco, C., Flessati, L., Frigerio, G., Galli, A.: Mathematical modelling of the mechanical response of earth embankments on piled foundations. Geotechnique **70**(9), 755–773 (2020). https://doi.org/10.1680/jgeot.18.P.127

19. Itasca.: FLAC3D v.5.0—Fast Lagrangian analysis of continua in three dimensions. User manual. Itasca Consulting Group, Minneapolis. Minneapolis (2012)
20. Flessati, L., di Prisco, C., Corigliano, M., Mangraviti, V.: A simplified approach to estimate settlements of earth embankments on piled foundations: the role of pile shaft roughness. Eur. J. Environ. Civil Eng. (2022). https://doi.org/10.1080/19648189.2022.2035259
21. Mangraviti, V., Flessati, L., di Prisco, C.: Geosynthetic-reinforced and pile-supported embankments: theoretical discussion of finite difference numerical analyses results. Under Rev. (2022)
22. Koerner, G.R.: Relative sustainability (i.e., Embodied Carbon) calculations with respect to applications using traditional materials versus geosynthetics. Geosynthetic Institute (2019)
23. Raja, J., Dixon, N., Fowmes, G., Frost, M., Assinder, P.: Obtaining reliable embodied carbon values for geosynthetics. Geosynth. Int. **22**(5), 393–401 (2015). https://doi.org/10.1680/jgein.15.00020